

Journal of Biomedical Optics

SPIEDigitalLibrary.org/jbo

***In vivo* high spatiotemporal resolution visualization of circulating T lymphocytes in high endothelial venules of lymph nodes**

Kibaek Choe
Yoonha Hwang
Howon Seo
Pilhan Kim



SPIE

In vivo high spatiotemporal resolution visualization of circulating T lymphocytes in high endothelial venules of lymph nodes

Kibaek Choe, Yoonha Hwang, Howon Seo, and Pilhan Kim

Korea Advanced Institute of Science and Technology (KAIST), Graduate School of Nanoscience and Technology (WCU), 291 Deahak-ro, Yuseong-gu, Daejeon, 305-701, Republic of Korea

Abstract. Lymph nodes (LN) are major checkpoints for circulating T lymphocytes to recognize foreign antigens collected from peripheral tissue. High endothelial venule (HEV) in LN facilitates the effective transmigration of circulating T lymphocytes from the blood into LN. There have been many efforts to visualize T lymphocytes trafficking across HEV to understand the underlying mechanism. However, due to insufficient spatiotemporal resolution and the lack of an *in vivo* labeling method, clear visualization of dynamic behaviors of rapidly flowing T lymphocytes in HEV and their transmigration have been difficult. In this work, we adapted a custom-designed video-rate laser scanning confocal microscopy system to track individual flowing T lymphocytes in the HEV in real time *in vivo*. We demonstrate that the HEVs in LN can be clearly identified *in vivo* with its distinctive cuboidal morphology of endothelial cells fluorescently labeled by intravenously injected anti-CD31 antibody conjugated with Alexa fluorophore. By visualizing the adaptively transferred T lymphocytes, we successfully analyzed dynamic flowing behaviors of T lymphocytes and their transendothelial migration while interacting with the endothelial cells in HEV. © The Authors. Published by SPIE under a Creative Commons Attribution 3.0 Unported License. Distribution or reproduction of this work in whole or in part requires full attribution of the original publication, including its DOI. [DOI: [10.1117/1.JBO.18.3.036005](https://doi.org/10.1117/1.JBO.18.3.036005)]

Keywords: lymph node; high endothelial venule; lymphocytes; confocal microscopy; intravital microscopy.

Paper 12803R received Dec. 18, 2012; revised manuscript received Feb. 13, 2013; accepted for publication Feb. 14, 2013; published online Mar. 5, 2013.

1 Introduction

To achieve an effective immune surveillance over wide area of human body, the immune system is operated by highly mobile lymphocytes. Lymph nodes (LN) are small nodular tissues encapsulating numerous lymphocytes, and which are distributed throughout the body. LN continuously collect interstitial fluid from peripheral tissues via lymph vessels. At the same time, foreign antigens are drained to LN either in soluble form or by antigen presenting cells, which makes LN an ideal place for T lymphocytes to recognize them. Due to the low frequency of naïve T lymphocytes for any specific antigen, a huge population of T lymphocytes constantly recirculates LN over the body via the blood and lymph network to ensure prompt induction of immune response. To facilitate the effective recruitment of T lymphocytes from the blood to LN, a specialized blood vessel called high endothelial venule (HEV)¹⁻³ exists in LN. Notably, the transmigration across HEV is highly regulated to be allowed exclusively for lymphocytes, not for other types of circulating cells such as red blood cells (RBCs). The endothelial cells constituting an innermost layer of the HEV are directly exposed to the rapid blood flow while interacting with flowing lymphocyte to recruit them. For the last decade, several intravital imaging studies have documented the contribution of various adhesion molecules involved in lymphocyte trafficking across HEV.⁴⁻⁷ It has been shown that naïve T lymphocytes express a surface receptor L-selectin, which can bind

to peripheral node addressin (PNAd) expressed on the endothelial cells of HEVs. And the initial attachment of T lymphocytes to the endothelial cell and subsequent rolling behavior are L-selectin dependent. Despite the improved understanding of molecular mechanisms, the dynamic behaviors of rapidly flowing T lymphocytes interacting with the endothelial cells under shear condition in HEV have not been analyzed. In addition, transmigration of T lymphocytes across HEV endothelial cells in LN has not been clearly visualized *in vivo* although the transendothelial migration of neutrophils^{8,9} or leukocytes trafficking¹⁰ in peripheral tissues has been recently visualized *in vivo*. Insufficient spatiotemporal resolution of common intravital imaging system to distinguish individual flowing T lymphocytes and the endothelial cells simultaneously and, more critically, the lack of appropriate *in vivo* labeling method for the endothelial cells in HEVs are major technical challenges to achieve their visualization.

In this work, to track individual flowing T lymphocytes *in vivo* and dissect their dynamic interactions with HEV endothelial cells in real time, we adapted a previously reported custom-designed video-rate laser scanning confocal microscopy system capable of three color fluorescence image acquisition at the speed of 30 frames per seconds in sub-micron resolution.^{11,12} Intravenous injection of anti-CD31 [also known as platelet endothelial cell adhesion molecule (PECAM-1)] monoclonal antibody conjugated with green fluorophore, Alexa Flour 488, allowed us to visualize the endothelial cells of HEV as those have a distinctive tall and plump shape. With careful surgical opening of skin and fascia at popliteal fossa of an anesthetized mouse, we successfully identified multiple HEVs in a popliteal lymph node (PLN) *in vivo*. To examine dynamic

Address all correspondence to: Pilhan Kim, Korea Advanced Institute of Science and Technology (KAIST), Graduate School of Nanoscience and Technology (WCU), 291 Deahak-ro, Yuseong-gu, Daejeon, 305-701, Republic of Korea. Tel: 82-42-350-1115; Fax: 82-42-350-1110; E-mail: pilhan.kim@kaist.ac.kr

behaviors of circulating T lymphocytes while interacting with endothelial cells in the HEV labeled with green fluorophore, Alexa Flour 488, we adaptively transferred T lymphocytes labeled by orange fluorophore, CMTMR. In addition, RBCs labeled by crimson fluorophore, DiD, that does not interacting with the endothelial cells were transferred simultaneously to compare flowing behaviors of T lymphocytes and RBC. With video-rate image acquisition in submicron resolution, it was observed that flowing cells dramatically slowed down at the moment they enter the large lumen of HEV from capillaries with smaller diameter, which provides T lymphocytes with more time to interact with endothelial cells of HEV. Interestingly, in some capillaries, T lymphocytes slowed down even before entering the HEV compared to RBC, suggesting additional mechanism to assist T lymphocytes to interact with endothelial cells of HEV. Subsequently, most T lymphocytes slowly flowed along the endothelial cells in HEV (rolling) while RBC rapidly passed in a pattern evenly distributed in the HEV lumen, which is demonstrated by generating high resolution velocity-color map in HEV and connected capillaries. Followed by the rolling behavior, some T lymphocytes adhered to the endothelial cell of HEV (sticking), then either proceeded to transendothelial migration or detached to flow again. Notably, some T lymphocytes repeat the sticking and detaching before finally adhered to certain endothelial cells to proceed to transendothelial migration. By acquiring the time-lapse imaging, for the first time to our knowledge, the paracellular transendothelial migration of T lymphocytes squeezing between plump endothelial cells of HEV was clearly visualized *in vivo*.

2 Materials and Methods

2.1 Imaging System

A video-rate laser scanning confocal microscopy system was implemented by adapting a previously developed confocal imaging platform.^{11,12} Figure 1 depicts the schematic of the optical setup for imaging. Beam path of excitation beam and emitted fluorescence were marked by solid and dashed line, respectively.

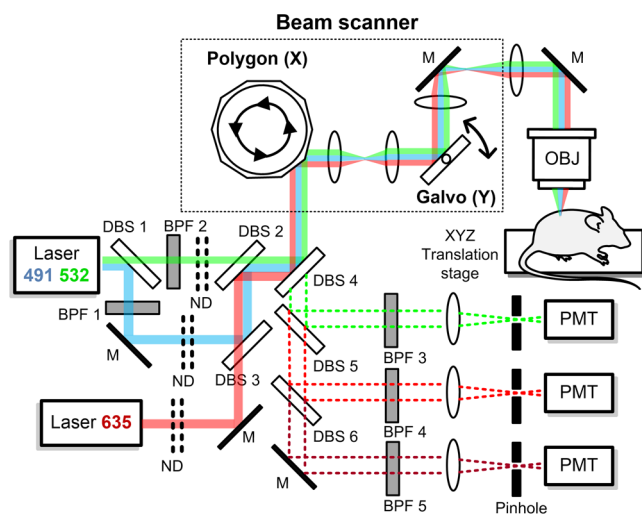


Fig. 1 Schematic of intravital imaging system based on a custom-built video-rate laser scanning confocal microscope platform: DBS, dichroic beam splitter; BPF, band pass filter; M, mirror; PMT, photomultiplier tube; OBJ, objective lens.

Three laser lines, constituted by dual-wavelength output DPSS laser emitting at 491 and 532 nm (Dual Calypso, Cobolt) and HeNe laser emitting at 635 nm (Radius, Coherent) were used as excitation lights for fluorescence imaging. To adjust power independently, dual-wavelength beams of 491 and 532 nm emitted from a DPSS laser were split to a single-wavelength beam by a dichroic beam splitter (DBS1; FF520, Semrock) and bandpass filters (BPF1; FF01-494/20, BPF2; FF01-531/22, Semrock). All three wavelength beams were combined by DBS2 (FF500/646, Semrock) and DBS3 (FF520, Semrock). Fast X-axis beam scanning at 17.28 kHz was achieved by rotating aluminum-coated polygon mirror (MC-5, Lincoln Laser). Combined with slow Y-axis beam scanning at 30 Hz achieved by a galvanometer-based scanner (6230H, Cambridge Technology), a two-dimensional raster beam scanning pattern was made and delivered to the back aperture of objective lens. Relaying lenses were selected to result in field of views (FOVs) of 1000×1000 , 250×250 and $125 \times 125 \mu\text{m}$ with $10\times$, $40\times$, and $60\times$ objective lens, respectively [UPlanFLN, numerical aperture (NA) 0.3; LUCPlanFI, NA 0.6; LUMFLN, water immersion, NA 1.1, Olympus]. The emitted fluorescence signals captured by the objective lens were de-scanned by back-propagating beam scanners. Then, multi-color fluorescence signals were separated from the excitation beams by DBS4 (FF494/540/650, Semrock) and split into three single color fluorescence signals by dichroic beam splitters (DBS5; FF555, Semrock, DBS6; FF650, Semrock) and bandpass filters (BPF3; FF01-512/25, BPF4; FF01-579/34, BPF5; FF01-676/29, Semrock). Three photomultiplier tubes (PMT; R9110, Hamamatsu) were used to detect the fluorescence signals, which were then digitized by an 8-bit 3-channel frame grabber (Solios, Matrox) at the speed of at ten million samples per second. Images were displayed at 512×512 pixels per frame at a frame rate of 30 Hz and stored in a hard disk in real time by using custom-written software based on Matrox Imaging Library (MIL9, Matrox).

2.2 Animal and Surgical Preparation

BALB/c mice aged eight weeks were used. Mice were anesthetized by intraperitoneal injection of xylazine (11 mg/kg) and ketamine (88 mg/kg). The level of anesthetization was continuously monitored during experiment by toe pinch and maintained by intramuscular injection with half dose xylazine-ketamine mixture whenever the response was observed. The popliteal fossa and surrounding skin area were shaved by hair clipper and hair removal cream. The PLN was surgically exposed by making small incision of skin and fascia at the popliteal fossa. To obtain clear view for the imaging, a fatty tissue covering the PLN was carefully removed by micro-dissection forceps. During the entire intravital imaging, the PLN was maintained at 37°C with warm saline and heat pad. Animal care and all experiments were performed with the approval of the Animal Care Committee of KAIST (protocol no. KA2011-08).

2.3 Fluorescent Labeling

To visualize the endothelial cells in the HEV, they were labeled *in vivo* by intravenous injection of anti-CD31 monoclonal antibody (553370, BD) conjugated with Alexa488 (A20000, Invitrogen). About $25 \mu\text{g}$ of conjugated antibody was injected into the lateral tail vein 6 h before imaging. To visualize the flowing T lymphocytes in the HEV, they were isolated from the dissected spleen of BALB/c mouse and fluorescently labeled *ex vivo*. With a negative

T lymphocytes isolation kit (114.13D, Invitrogen), untouched T lymphocytes were isolated with high purity by depleting non-T lymphocytes. Higher than 97% purity of isolated T lymphocytes was confirmed by FACS analysis using pan-T lymphocytes marker CD3e. Isolated T lymphocytes were fluorescently labeled by 5-(and-6)-(((4-chloromethyl)benzoyl)amino) tetramethylrhodamine (CMTMR; C2927, Invitrogen). Likewise T lymphocytes, to visualize the flowing RBCs in the HEV, 20 μ l of blood was drawn from retro-orbital sinus of anesthetized mouse and fluorescently labeled with DiD (V-22887, Invitrogen). Labeled T lymphocytes and RBCs were transferred to anesthetized mouse under imaging by intravenous injection into the lateral tail vein.

2.4 Image Processing and Data Analysis

Signal to noise ratio (SNR) and contrast of image were enhanced by averaging the noise over multiple frames and adjusting image intensity values with Matlab (Mathworks), respectively. In video-rate (30 frame/s) real-time movie showing the dynamic flow of T lymphocytes and RBC inside HEV, green channel was averaged over 30 frames (1 s) to enhance the contrast of endothelial cells labeled by green fluorophore, Alexa488. A time-lapse movie showing the transendothelial migration of T lymphocyte was generated by averaging 30 frames (1 s, red) or 90 frames (3 s, green) to 1 frame. Two images obtained at different depth are merged to clearly show endothelial cells lining HEV and the connected capillaries those are located in different depth. The manual tracking plugin for ImageJ (National Institutes of Health) was used to track the individual cell movements and quantify the average and temporal velocity. The velocity-time graph and velocity colormap were generated by Matlab.

3 Results

3.1 *In Vivo* Visualization of T Lymphocytes Interacting with Endothelial Cells in HEV of Lymph Nodes

Figure 2(a) shows whole left PLN at 1 h after the intravenous injection of T lymphocytes fluorescently labeled by CMTMR (red) and RBCs labeled by DiD (blue). The number of injected T lymphocytes and RBCs are 3×10^7 and 2×10^7 , respectively. Endothelial cells lining blood vessels were fluorescently labeled by Alexa488-conjugated anti-CD31 antibody (green). Multiple post-capillary HEVs are easily distinguishable from capillary with their much larger lumen than capillaries. Only after 1 h, numerous T lymphocytes were found to be accumulated around the HEVs and several T lymphocytes were already visible inside the LN through transmigration across HEV endothelial cells. Dotted and solid squares in Fig. 2(a) indicate the area shown in magnified scale in Fig. 2(b) and 2(c), respectively. Figure 2(b) shows the complex structure of the HEV with six entrances connected with 1 to 3 capillaries each. As a post-capillary venule, blood flows into the HEV from the six entrances then flows out to single downstream collecting venule (Video 1). Complex curved shapes in HEV may help T lymphocytes contact to endothelial cells more frequently. Individual HEV-endothelial cells have plump and cuboidal shape that were clearly visible in higher magnification [Fig 2(c)], which makes them easily distinguishable from endothelial cells of normal capillaries as those have a flat shape. T lymphocytes were attached to the plump endothelial cells for a short period

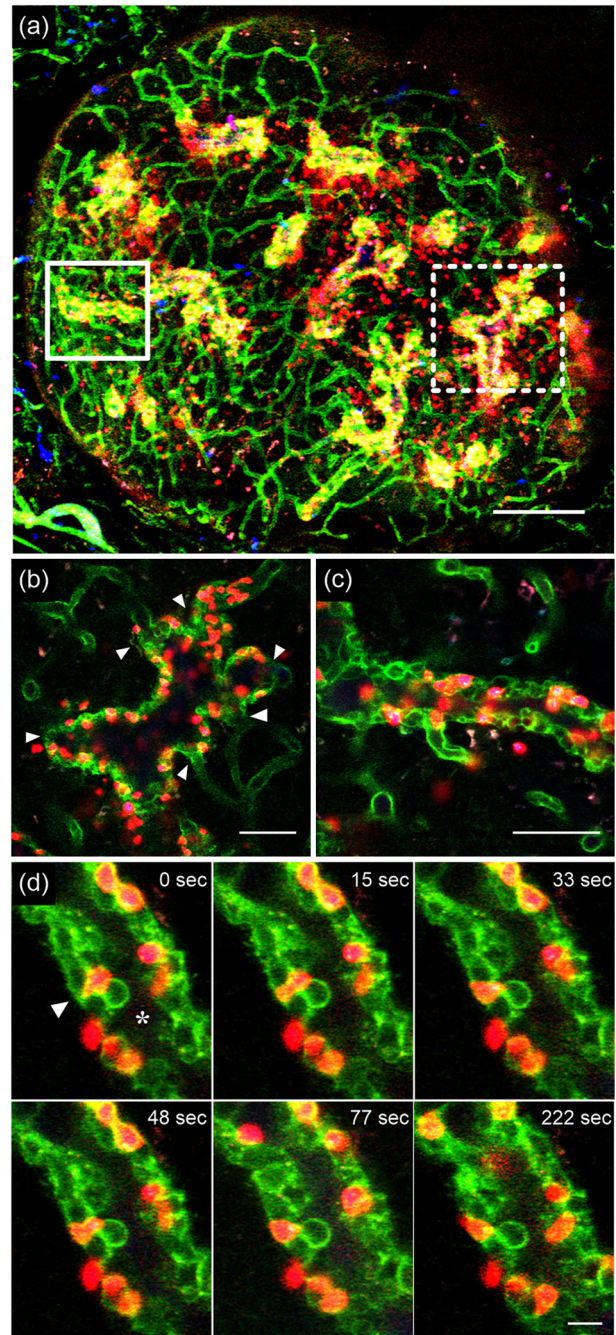


Fig. 2 Intravital images of T lymphocytes and vascular endothelial cells in HEVs of the PLN. (a) Mosaic image of whole PLN showing distribution of CMTMR-stained T lymphocytes (red) and CD31+ vasculature (green) in the cortical side of the PLN at 1 h after the transfer of T lymphocytes. The number of injected T lymphocytes is 3×10^7 . (b) and (c) Magnified images of the area marked by dotted and solid lines in (a) those indicate (b) and (c), respectively. (b) T lymphocytes enter complex shaped HEV from six entrances (arrowhead) connected with capillaries and adhere to endothelial cells (green) (Video 1). (c) Individual HEV-endothelial cells having distinctive plump morphology are distinguishable and prolonged rolling behavior of T lymphocytes interacting with endothelial cells are observed (Video 2). (d) Paracellular transmigration of T lymphocyte across endothelial cells in HEV (Video 3). Star indicates the lumen of the HEV. Scale bars are (a) 200 μ m, (b) and (c) 50 μ m and (d) 10 μ m (Video 1, QuickTime, 6.32 MB, [URL: <http://dx.doi.org/10.1117/1.JBO.18.3.036005.1>]; Video 2, QuickTime, 9.88 MB, [URL: <http://dx.doi.org/10.1117/1.JBO.18.3.036005.2>]; Video 3, QuickTime, 2.54 MB, [URL: <http://dx.doi.org/10.1117/1.JBO.18.3.036005.3>]).

time and detached from them in a repetitive manner, a distinctive rolling behavior, while RBCs passed by rapidly (Video 2). On the other hand, some T lymphocytes firmly adhered in endothelial cells started to transmigrate across the endothelial cells from the lumen of HEV [Fig. 2(d) and Video 3]. The T lymphocyte started to squeeze in to the space between endothelial cells of HEV and passed through in less than 2 min. In previous studies *in vitro*,¹³ two routes those T lymphocytes can take during transendothelial migration were identified: paracellular and transcellular migration.¹⁴ Paracellular migration refers the passing through the junction between endothelial cells as shown in Fig. 2(d) while transcellular refers intraendothelial passage. Figure 2(d) shows, for the first time to our knowledge, clear paracellular migration of T lymphocytes in HEV *in vivo* in real-time, which is enabled by *in vivo* labeling of endothelial cell of HEV by anti-CD31 antibody conjugated with Alexa488. The T lymphocytes are marked by arrowhead.

3.2 Characterization of Circulating T Lymphocyte Behaviors in Post-Capillary HEV

Previous studies have identified distinctive T lymphocytes behaviors inside HEV: rolling and sticking. Rolling refers T lymphocytes flowing slowly along endothelium at lower than a certain predetermined critical velocity and sticking refers firm adhesion of T lymphocytes to endothelium for 30 s at least.¹⁵ Figure 3 and Video 4 show real-time tracking result of rolling and sticking behaviors of individual T lymphocytes and RBCs inside HEV, which is enabled by video-rate confocal imaging system implemented in this work. Highly dynamic behaviors of T lymphocytes associated with endothelial cells of HEV can be dissected in high spatiotemporal resolution. Figure 3(a) shows selected frames obtained in video-rate 30 frames per second in which the tracks of individual flowing cells were marked by colored lines. Three distinctive dynamic behaviors of T lymphocytes, flowing (red, dotted line), rolling (green, solid line) and sticking (magenta, dotted line) were shown. Real-time velocity changes of T lymphocytes after entering into HEV from capillaries at time zero are shown in Fig 3(b). For comparison, the velocity change of RBCs was also shown (blue, solid line). The velocities of all flowing cells dramatically decreased to $\sim 100 \mu\text{m/s}$ at zero time when they encountered large space of the HEV [Fig. 3(b)]. Flowing T lymphocyte (red) passed through the HEV within 1 s as fast as RBC (blue). On the other hand, rolling T lymphocytes (green) started to slowly roll along the endothelium just after entered the HEV. At 1.6 s, rolling T lymphocyte detached from the endothelium and quickly reached flowing speed as fast as RBC, then abruptly stopped flowing at 1.9 s. Subsequently the T lymphocyte adhered to endothelial cell for 0.83 s [from 3.896 to 4.729 s in Fig. 3(a)]. Sticking T lymphocytes (magenta) initially stopped flowing for 0.9 s and slowly rolled for 0.2 s with average speed slower than $30 \mu\text{m/s}$, then finally firmly adhered to endothelium for more than 30 s. Although the time-velocity graph is useful to dissect temporal dynamics of individual flowing cell, it does not provide information about the spatial distribution of velocity changes in HEV with complex structure. Velocity colormaps presenting the both of spatial and temporal information of the velocity of flowing T lymphocyte and RBCs in the HEV were generated (Fig. 4). More than 20 individual T lymphocytes and RBCs from two capillaries were tracked and instantaneous velocities were measured. Likewise the time-velocity graph [Fig. 3(b)], the velocity of both T

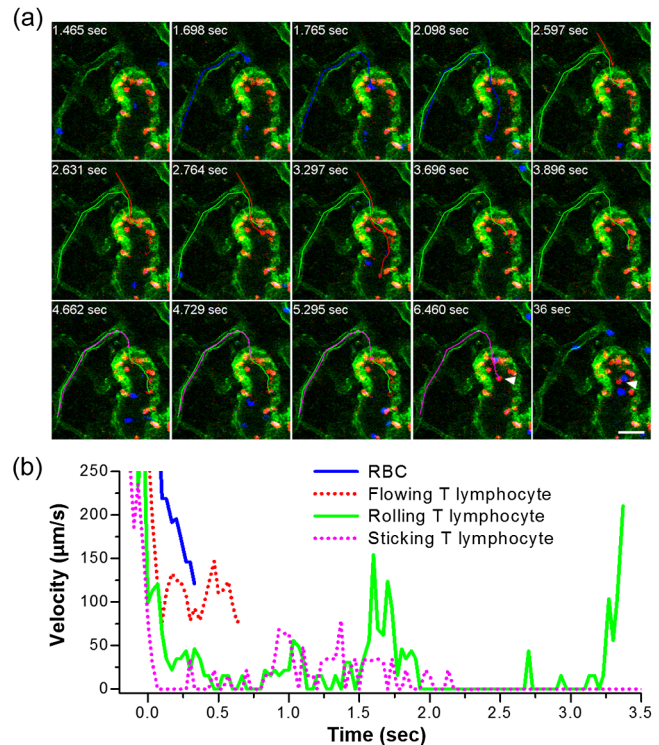


Fig. 3 Tracking of rapidly flowing individual T lymphocyte interacting with endothelial cells in post-capillary HEV. (a) Real-time frames showing tracks of individual cell of which colors match the corresponding lines in time-velocity graph (b) (Video 4). Arrowhead points the firmly adhered T lymphocyte that is immobile for at least 30 s. (b) Time-velocity graph shows the velocity changes of T lymphocytes showing representative behaviors of rolling, sticking and flowing in the HEV, as well as flowing RBCs for comparison. Zero time indicates when each cell enters the HEV from capillaries. Scale bar is $30 \mu\text{m}$ (Video 4, QuickTime, 8.24 MB) [URL: <http://dx.doi.org/10.1117/1.JBO.18.3.036005.4>].

lymphocytes and RBCs dramatically decreased at the very moment when they entered the HEV [Fig. 4(c)]. To highlight small velocity changes inside HEV those are slower than $200 \mu\text{m/s}$, we generated normalized velocity colormaps [Fig. 4(d)], which shows much detailed dynamic change of T lymphocyte velocity in the HEV. Tracks of flowing RBCs inside HEV are evenly distributed over entire lumen of the HEV and the velocities of RBCs seem to slow down more as they further flows inside HEV. In contrast, the tracks of flowing T lymphocytes were divided into left and right toward the endothelial cells just after they entered the HEV. This shift of the flowing track of T lymphocytes toward the endothelial cell when they moved into a venule with larger lumen from capillary has been expected by *in vitro* modeling.^{16,17} It has been suggested that the accumulated RBCs behind slowly flowing T lymphocyte in narrow capillary can thrust the T lymphocyte toward endothelial cell when they enter the large lumen. And this can be a critical step to initiate the rolling of T expressing surface receptor L-selectin that bind to PNA_d expressed on the endothelial cells of HEVs. We believe, to the best of our knowledge, that this is the first time to directly visualize this shifted flowing track of T lymphocyte inside HEV of LN in real time *in vivo*. On the other hand, these distinctive shifted flowing tracks of T lymphocytes might be also caused by the centrifugal force due to the curved shape of endothelium. Nevertheless,

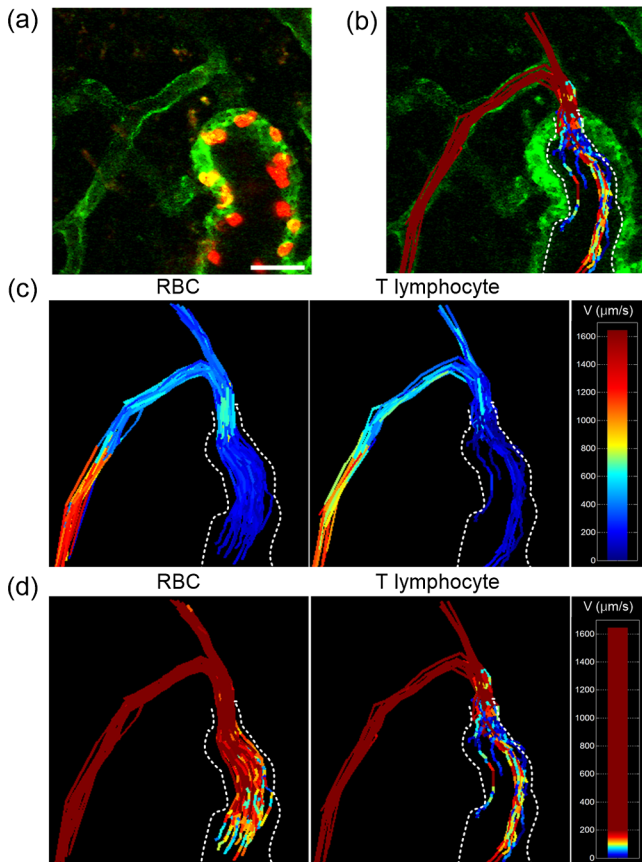


Fig. 4 *In vivo* high spatiotemporal resolution tracking of flowing RBCs and T lymphocytes in the post-capillary HEV. (a) Image of endothelial cell (green) of HEV and connected capillaries. Adhered T lymphocytes (red) were visible. (b) Image of vascular structure overlaid with velocity colormaps of T lymphocytes shown in (d). (c) Velocity colormaps of RBCs and T lymphocytes showing the changing velocity of individual flowing cells in HEV and spatial distribution of them simultaneously. The lumen lined by endothelial cells of HEV is delineated by dotted white lines. (d) Normalized velocity colormaps to $200 \mu\text{m/s}$ to clearly show small velocity change in HEV. Scale bar is $30 \mu\text{m}$.

T lymphocytes flowing along the curved endothelium of HEV would have more chance to interact with endothelial cells and subsequently proceed to extravagate into LN, which facilitate the efficient recruitment of T lymphocyte to ensure the prompt induction of immune response against potential antigen collected to the LN.

3.3 Initiation of T Lymphocyte Interaction with Endothelial Cells in Post-Capillary HEV

Initiation of rolling along endothelial cell is the first critical step in T lymphocyte adhesion cascades for the recruitment of T lymphocytes to peripheral LN. As mentioned above, repetitive change of blood flow direction by complex curved shape of the HEV may provide frequent contact of T lymphocyte with endothelial cells. This complex shape was observed in post-capillary HEV more frequently in comparison with general downstream venules. This partially explains why rolling fraction is significantly larger in post-capillary HEVs compared with downstream venules.⁴ Significantly larger lumen of HEV compared to the connected capillary also aids to contribute the initiation of rolling since it makes flow velocity to decrease rapidly when the flowing T lymphocytes encounter the large lumen of HEV. As mentioned before, previous studies suggested rapidly flowing upstream RBCs may push T lymphocytes to endothelium when they enter the HEV with increased diameter, which can initiate the interaction between them.^{16,17} As shown in Fig. 4, RBCs in the capillary connected with HEV were slightly faster than T lymphocytes due to their smaller sized disk shape and larger elastic deformation during flow in narrow blood vessels, which could lead to RBC accumulation upstream of T lymphocyte and pushing T lymphocytes to endothelium when they encounter the large lumen of HEV.

In this work we newly observed that T lymphocyte started to slow down in some capillaries before entering the HEV. Velocity-time analyses of flowing T lymphocytes and RBCs performed in two independent HEVs, named as HEV1 and HEV2, are shown in Fig. 5(a) and 5(c). For each HEV, more than 20

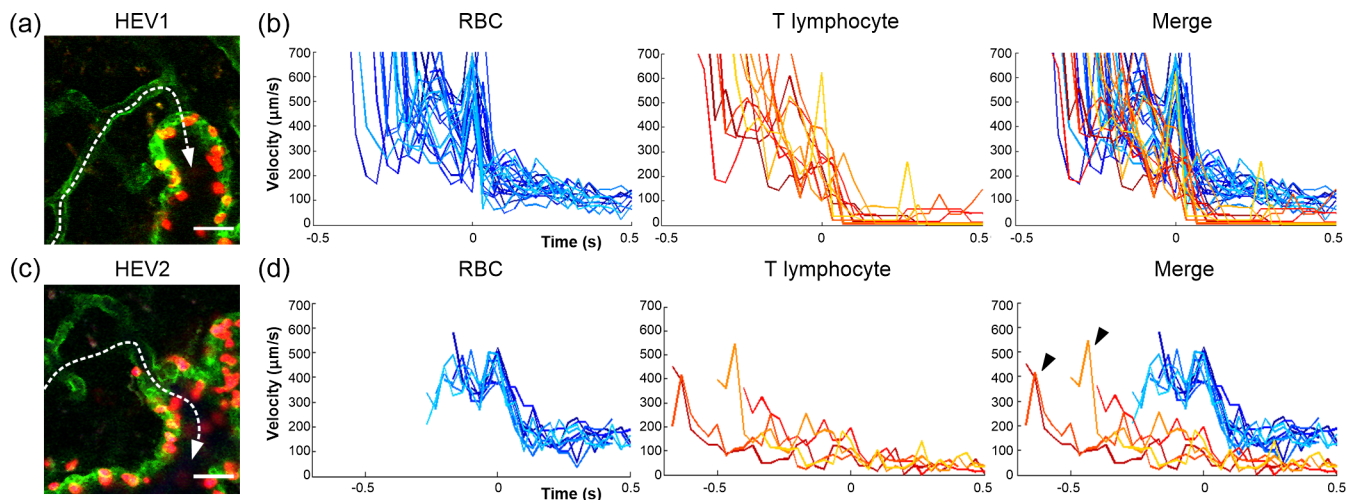


Fig. 5 Detailed tracking of the initiation of T lymphocyte rolling. (a) Image of HEV1 and the connected capillary. The flow path of analyzed cells is marked by a dotted white line. (b) Time-velocity graphs showing the velocity changes of RBCs (blue) and T lymphocytes (red) in HEV1. Zero time indicates when the cells enter the HEV from the connected capillary. (c) Image of HEV2 and the connected capillary. (d) Time-velocity graphs of RBCs (blue) and T lymphocytes (red) in HEV2. T lymphocytes those flowed as fast as RBC (arrowheads) started to slow down at the capillary before entering HEV2. Scale bar is $30 \mu\text{m}$.

flowing cells were tracked and velocity-time graphs were generated [Fig. 5(b) and 5(d)]. To clearly distinguish the flowing dynamics of cells before entering HEV, all of velocity-time tracks were aligned such that the exact moment when cells enter the HEV should be time zero. Velocity difference between RBCs and T lymphocytes in the pre-HEV2 capillary [Fig. 5(d)] is much larger than that in the pre-HEV1 capillary [Fig. 5(b)]. However, sizes of connected capillaries of HEV1 and HEV2 were not significantly different, 10 μm and 11 μm , respectively, and sufficiently larger than the average size of T lymphocytes (6 to 7 μm). Some T lymphocytes in pre-HEV2 capillary slowed down to 8% of RBC velocity as they approached the HEV within about 100 μm . To note, before slowing down, they flowed as fast as RBC as shown in Fig. 5(d) (arrowheads). It suggests that there exists some adhesive force between T lymphocytes and the pre-HEV capillary endothelial cells in the vicinity of HEV.

4 Conclusion

In this study, we visualized rapidly flowing individual T lymphocytes in the HEV of LN *in vivo* by custom-built video-rate confocal microscopy system. With high spatiotemporal resolution, we directly tracked the distinctive behaviors of T lymphocytes, rolling and subsequent adhesion to endothelial cells of HEV, and analyzed their fast dynamics compared with RBCs by generating velocity colormaps. We demonstrated that the endothelial cells of HEV having distinctive plump morphology can be fluorescently labeled *in vivo* by intravenous injection of anti-CD31 antibody conjugated with Alexa fluorophore, which enables the clear visualization of T lymphocyte transmigration between endothelial cells in HEV *in vivo*, for the first time to our knowledge. These methods can help future studies to investigate the dynamics of lymphocytes in the HEV of LN of murine model by enabling direct monitoring of their behavior *in vivo*, which can contribute to improve our understanding about the cellular mechanism of lymphocytes in normal and pathophysiological conditions, such as infection or cancer.

Acknowledgments

The authors thank Raghu P. Kataru and Gou Young Koh at Korea Advanced Institute of Science and Technology (KAIST) for valuable discussions and technical help on the preparation of T lymphocyte. This work was supported by the World Class Institute program (WCI 2011-001), the World Class University program (WCU R31-10071), the Engineering Research Center program (2011-0009503), the Global Frontier Project (NRF-M1AXA002-2012M3A6A4054261) of National Research Foundation of Korea and the Converging Research Center Program (2011K000864) funded by the

Ministry of Education, Science and Technology, and the Korea Healthcare Technology R&D Project (A103017) funded by Ministry of Health and Welfare.

References

1. H. Hayasaka et al., "Neogenesis and development of the high endothelial venules that mediate lymphocyte trafficking," *Cancer Sci.* **101**(11), 2302–2308 (2010).
2. M. Miyasaka and T. Tanaka, "Lymphocyte trafficking across high endothelial venules: Dogmas and enigmas," *Nat. Rev. Immunol.* **4**(5), 360–370 (2004).
3. U. H. von Andrian and T. R. Mempel, "Homing and cellular traffic in lymph nodes," *Nat. Rev. Immunol.* **3**(11), 867–878 (2003).
4. R. A. Warnock et al., "Molecular mechanisms of lymphocyte homing to peripheral lymph nodes," *J. Exp. Med.* **187**(2), 205–216 (1998).
5. A. van Zante et al., "Lymphocyte-HEV interactions in lymph nodes of a sulfotransferase-deficient mouse," *J. Exp. Med.* **198**(9), 1289–1300 (2003).
6. R. T. Boscacci et al., "Comprehensive analysis of lymph node stroma-expressed Ig superfamily members reveals redundant and nonredundant roles for ICAM-1, ICAM-2, and VCAM-1 in lymphocyte homing," *Blood* **116**(6), 915–925 (2010).
7. E. J. Park et al., "Distinct roles for LFA-1 affinity regulation during T-cell adhesion, diapedesis, and interstitial migration in lymph nodes," *Blood* **115**(8), 1572–1581 (2010).
8. A. Woodfin et al., "The junctional adhesion molecule JAM-C regulates polarized transendothelial migration of neutrophils *in vivo*," *Nat. Immunol.* **12**(8), 761–769 (2011).
9. D. Proebstl et al., "Pericytes support neutrophil subendothelial cell crawling and breaching of venular walls *in vivo*," *J. Exp. Med.* **209**(6), 1219–1234 (2012).
10. C. Q. Li et al., "Imaging leukocyte trafficking *in vivo* with two-photon-excited endogenous tryptophan fluorescence," *Opt. Express* **18**(2), 988–999 (2010).
11. P. Kim et al., "*In vivo* wide-area cellular imaging by side-view endomicroscopy," *Nat. Methods* **7**(4), 303–305 (2010).
12. I. Veilleux et al., "*In vivo* cell tracking with video rate multimodality laser scanning microscopy," *IEEE J. Sel. Top. Quant. Electron.* **14**(1), 10–18 (2008).
13. C. V. Carman and T. A. Springer, "A transmigratory cup in leukocyte diapedesis both through individual vascular endothelial cells and between them," *J. Cell Biol.* **167**(2), 377–388 (2004).
14. B. Engelhardt and H. Wolburg, "Mini-review: transendothelial migration of leukocytes: through the front door or around the side of the house?," *Eur. J. Immunol.* **34**(11), 2955–2963 (2004).
15. C. Halin et al., "*In vivo* imaging of lymphocyte trafficking," *Annu. Rev. Cell Dev. Biol.* **21**(1), 581–603 (2005).
16. G. W. Schmid-Schonbein et al., "The interaction of leukocytes and erythrocytes in capillary and postcapillary vessels," *Microvasc. Res.* **19**(1), 45–70 (1980).
17. C. H. Sun, C. Migliorini, and L. L. Munn, "Red blood cells initiate leukocyte rolling in postcapillary expansions: a lattice Boltzmann analysis," *Biophys. J.* **85**(1), 208–222 (2003).